



## The effect of coagulation time on the performance of thin film composite reverse osmosis membrane supported on nonwoven polyester fabric

Randa I. Gaber<sup>a,\*</sup>, A.H. Konsowa<sup>a</sup>, M.G. Eloffy<sup>a</sup>, Eman A. Fadl<sup>b</sup>, Sherif H. Kandil<sup>b</sup>

<sup>a</sup>Department of Chemical Engineering, Faculty of Engineering, Alexandria University, Lotfy El-Sied st. off Gamal Abd El-Naser – Alexandria, Alexandria Governorate 11432, Alexandria, Egypt, Tel. +201021076579; emails: randaibrahim2011@yahoo.com (R.I. Gaber), akonsowa@alex-eng.edu.eg (A.H. Konsowa); Tel. +201226150501; email: manal\_elfoffy@yahoo.com (M.G. Eloffy)

<sup>b</sup>Department of Materials Science, Institute of Graduate Studies and Research, Alexandria University, 163 Horreya Avenue, El-Shatby, P.O. Box 832, Alexandria, Egypt, Tel. +201225118271; email: eman\_fadl@yahoo.com (E.A. Fadl), Tel. +201003400746; email: s.kandil@usa.net (S.H. Kandil)

Received 30 May 2018; Accepted 27 December 2018

### ABSTRACT

This work aims to optimize the coagulation time for developing high-performance thin film composite polyamide reverse osmosis (TFC-PA-RO) membrane supported on nonwoven polyester fabric. A PA layer was synthesized by interfacial polymerization on the surface of polysulfone (PS) membrane. PS membrane was prepared by phase inversion technique. The effect of using two different types of nonwoven polyester fabric as support for the prepared membranes on their performance was investigated. The morphology of the prepared membranes was studied using scanning electron microscope. The performance (water flux and salt rejection) of the prepared RO membranes at different coagulation times (10, 30, 60, and 120 min) was compared with the standard RO membranes in 10 g L<sup>-1</sup> NaCl solution. The TFC-PA-RO membrane supported on nonwoven polyester and prepared at a coagulation time of 30 min exhibited a maximum water flux of 47.6 L m<sup>-2</sup> h<sup>-1</sup> and salt rejection of 98% at 55 bar. On the other hand, the standard seawater high-rejection flat sheet membrane showed a maximum water flux of 27 L m<sup>-2</sup> h<sup>-1</sup> and salt rejection of 97.9%.

*Keywords:* Membrane; Reverse osmosis; Thin film composite; Interfacial polymerization; Polysulfone

### 1. Introduction

Desalination has become an important process for effective water management; it can be seen as one of the most important solutions to overcome the increasing shortage in municipal water supply. About 54% of the global growth of water desalination is expected to occur in the Middle East and North Africa regions [1,2] and is expected to reach 110 million m<sup>3</sup> d<sup>-1</sup> by 2030 [3,4]. Like other membrane separation processes, reverse osmosis has the advantage of affecting the separation without the need for the creation of a second phase as in distillation, absorption, etc. Thus, no thermal energy or

separating agents are required, which makes the process economically attractive [5]. RO plants are now the most commonly installed desalination systems in the world, accounting for ~75% of the newly built capacity, except for areas with vast energy reserves or high-salinity feed water [6,7]. The thin film composite polyamide reverse osmosis (TFC-PA-RO) membrane offers many advantages such as high water molecule transport rate, excellent mechanical properties (under high pressure of seawater desalination applications), and relative stability over a wide range of pH [8]. TFC membranes consist of an ultrathin selective surface layer on a much thicker but much more permeable micro porous support, which produces the mechanical strength. These membranes are formed by the deposition of a PA layer via

\* Corresponding author.

interfacial polymerization (IP) on a porous PS support [9]. The PS support membrane is prepared by the phase inversion technique; this process involves the solidification (gelation) of the casted polymer solution that determines the final membrane morphology and the associated separation performance. The polymer concentration and the additives have a great effect on the support layer formation and the performance of the fabricated TFC membranes. It was noted that the morphology (i.e. structure, thickness, and surface charge) and the performance (i.e. permeability and selectivity) of a TFC membrane may be altered with the use of different substrate properties [10–13].

The microporous PS membrane, which acts as a support for the TFC membrane, should be smooth with high hydraulic permeability. The thickness of the PS membrane must be maintained as little as possible to decrease the resistance to the permeate transport, and at the same time, the membrane should stand a high operating pressure. Therefore, the nonwoven polyester fabric that has a high tear and tensile strength and chemical stability is used as a good mechanical backing layer to support the PS membrane [14].

The main factors determining the membrane behavior and performance in a filtration process are the structure, the chemical composition, and the operating conditions [15,16]. Therefore, the coagulation time is one of the significant parameters; it is considered as the time taken by the polymer solution film after being immersed into the coagulation bath till it reaches complete polymer solidification (including the time of diffusion of solvent and nonsolvent across the interface between the casting solution and the coagulation bath).

The focus of this study is to investigate the effect of the coagulation time on the morphology and the performance (salt rejection and water flux) of the TFC membranes supported on a nonwoven polyester fabric in comparison with the performance of the seawater high-rejection standard membrane.

## 2. Experimental work

### 2.1. Materials

Polysulfone (PS) pellets with molecular weight of 60,000, M-Phenylenediamine (MPD) (99%), and 1,3,5-Benzenetricarbonyl trichloride (TMC) (98%) were supplied by Acros Company, USA. N-Hexane (95%) was supplied by TEDIA Company, USA and the N-Methylpyrrolidone (NMP) was produced from Fisher Company, USA. Flat polyester nonwoven fabric PET/PBT (polyethyleneterephthalate – PET blended with polybutyleneterephthalate – PBT) with a thickness of 120  $\mu\text{m}$  (85  $\text{g m}^{-2}$ ) was purchased from Freudenberg Filtration Technologies Company, Germany, and a flat polyester (PET) spunbond nonwoven fabric with a thickness of 130  $\mu\text{m}$  (70  $\text{g m}^{-2}$ ) was purchased from Shouquang Huaya International Trade Company, China (Mainland). Dow Filmtech, SW30HR, as a Standard RO Flat Sheet Membrane, was purchased from Sterlitech Company, USA.

### 2.2. Methods

The PS solution was prepared by dissolving the pellets of PS (18 g) in NMP (72 mL) under vigorous stirring until

the complete dissolution was achieved. The solution was left overnight to remove the air bubbles.

#### 2.2.1. Preparation of PS membrane (without polyester support)

The bubble-free solution of PS was spread on a glass plate using an automatic film applicator (ZEHNTNER testing instruments ZAA2300, Swiss) with a thickness of 250  $\mu\text{m}$ . The glass plate that was covered with the PS solution was immersed in deionized water (DI) as a nonsolvent at room temperature until the PS membrane was separated from the glass plate. The PS membrane was washed and stored in DI for the preparation of the TFC-PA membrane by the IP.

#### 2.2.2. Preparation of PS supported on a nonwoven polyester fabric

Two commercial nonwoven polyester fabrics of PET/PBT and PET that differ in the thickness and the mechanical properties were used. The PS membrane which was prepared onto the polyester fabric without wetting with NMP was separated from the fiber. The polyester fabric was attached to a clean glass plate using a laboratory tape, wetted with NMP; the excess of NMP was allowed to drain by keeping the glass plate in a vertical position for 2 h. Pre-wetting process was applied to prevent the intrusion of the polymer solution inside the pores of the fabric and to keep the final thickness of the membrane as fixed and homogeneous as possible. Then, the casting solution was spread using an automatic film applicator with a thickness of 150  $\mu\text{m}$  over the polyester nonwoven fabric. After spreading the casting solution over the nonwoven fabric, the entire assembly was immediately immersed in a bath containing DI (as a nonsolvent) at room temperature. Phase inversion starts immediately, and the precipitated PS with the polyester films was removed from the water bath after various coagulation times (10, 30, 60, and 120 min). The membranes were then washed and stored in DI as shown in Fig. 1. The prepared PS membranes that were supported on nonwoven polyester of PET/PBT and PET were labeled as P1 and P2, respectively.

#### 2.2.3. Preparation of TFC membranes

The PS, P1, and P2 membranes immersed in DI overnight were removed from the water and positioned on a plastic plate with a rubber gasket and a plastic frame which was placed on top of it. Clips were used to hold the plate-membrane-gasket frame stacked together. MPD aqueous solution (2% w/v) was poured into the frame and was allowed to contact the support membrane for 2 min; then the excess of MPD was allowed to drain. This contact time allows the MPD solution to partially replace the DI water in the pores of the porous PS support. Residual droplets of the solution remaining on the top of the PS membrane surface were removed by using a rubber roller to prevent the defect formation onto the membrane surface. Afterward, TMC in *n*-hexane organic solution (0.1% w/v) was poured into the frame. After 1 min, the TMC/*n*-hexane solution was drained from the frame, and the frame and the gasket were disassembled. Then, the membranes were cured in an oven for 5 min

at 75°C and were left overnight in a dried dark place. Finally, the entire membrane sheets were immersed in DI water till used. Fig. 2 shows the schematic diagram of the TFC membrane preparation using typical IP technique, while Table 1 indicates the notations given to the prepared membranes.

#### 2.2.4. Characterization and testing

The surface morphology of the prepared membranes was studied using the scanning electron microscope (SEM) (Joel JSM 5300, Japan). The performance of the membranes was evaluated using a reverse osmosis system consisting of a cross-flow stainless steel cell CF042, with hydra cell pump (maximum pressure 69 bars) fitted with a pressure gauge, a control valve through the rejection line, and a flow meter F-550 (USA) to obtain a constant flow rate through the membrane area (42 cm<sup>2</sup>). The different components of the experimental setup are products of Sterlitech Corporation.

The performance of each membrane was tested at different operating pressures (35–60 bar).

### 3. Results and discussion

#### 3.1. The effect of the nonwoven polyester fabric on the morphology of PS membrane

SEM was used to investigate the morphological effect of using polyester as a support for the PS membrane. By immersing the PS solution in a nonsolvent, a phase separation occurs and propagates from the top surface of the wet film into the bulk. Fig. 3(a) shows the SEM image of a smooth surface of PS membrane. In the coagulation bath, the smooth surface layer of PS is formed due to outlet of NMP solvent and the precipitation of polymer. Therefore, the polymer concentration increases and becomes more viscous. This process continues until the polymer becomes

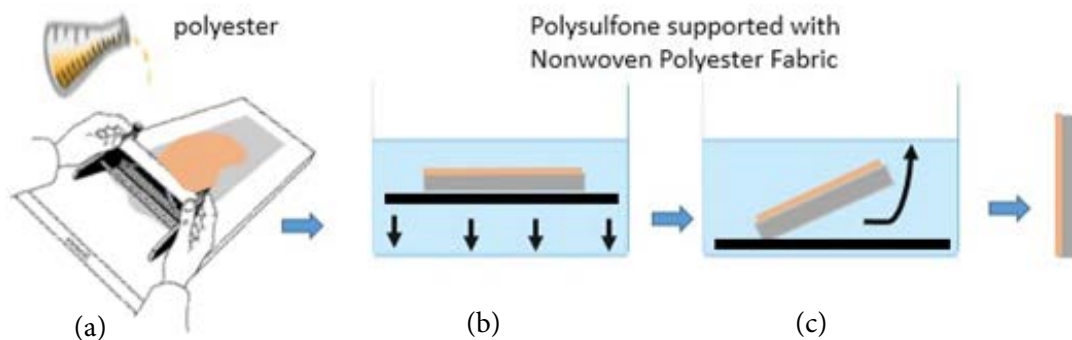


Fig. 1. Preparation steps of polysulfone membrane by the phase inversion technique on a nonwoven polyester fabric (a) casting the solution on polyester, (b) coagulation, and (c) washing and storage.

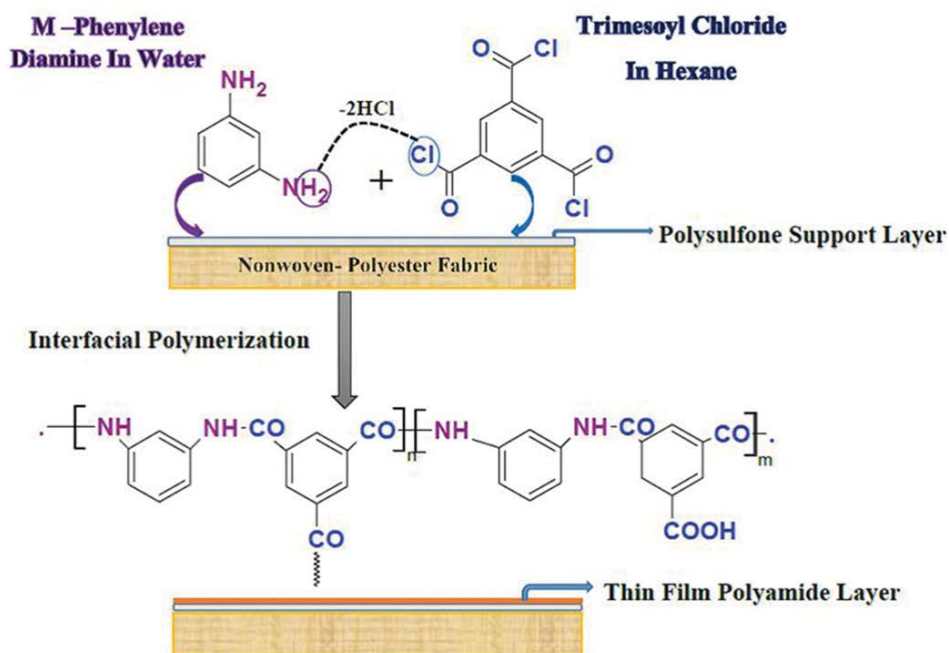


Fig. 2. Schematic diagram of interfacial polymerization technique for preparing the polyamide TFC membrane.

Table 1  
Notations for the prepared membranes

Entry	Membrane type	Notation
1	Thin film composite membrane without polyester	TFC
2	TFC supported on PET/PBT nonwoven polyester (P1)	TFC1
3	TFC supported only on PET nonwoven polyester (P2)	TFC2
4	Standard flat sheet RO membrane (SW30HR)	TFC-St

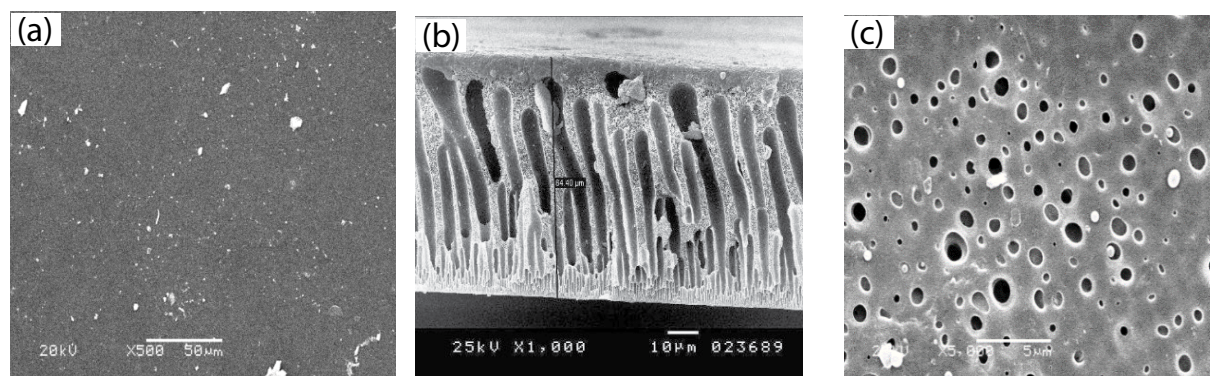


Fig. 3. SEM images of the PS membrane without the polyester: (a) top surface, (b) cross section, and (c) bottom.

almost solid forming dense layer at the surface [14]. Fig. 3(b) illustrates that the finger-like structure is produced as a result of unrevealed stresses that are formed due to the difference in the composition change of PS solution between the top and bottom surfaces. At the bottom, a little solvent diffuses out and little precipitant diffuses in; therefore, the bottom is porous as shown in Fig. 3(c).

It is noted that the thickness of the PS solution decreases after the immersion in DI, and this is attributed to the exchange between the solvent and the nonsolvent. Therefore, it is observed from the cross-sectional image that the PS thickness has decreased from 250  $\mu\text{m}$  as the applicator was adjusted to 64.4  $\mu\text{m}$  after immersion in DI.

Fig. 4 indicates that the whole cross section of the PS membrane is supported on nonwoven polyester fabric. It is found that the PS thickness supported on nonwoven polyester fabric has decreased from 150 (as the applicator was

adjusted) to 25  $\mu\text{m}$  after immersion in DI. Consequently, the polyester fabric as a backing layer is considered to augment the mechanical strength of PS.

Fig. 5 displays the bottom SEM images of the supported membranes (P1 and P2). These images show that the polyester fibers P2 are networked and overlapped with each other more than P1. On the other hand, Fig. 5(a) presents white lumps of PS onto the thinner polyester fibers of 4  $\mu\text{m}$ . These lumps were formed due to the penetration and physical interactions between PS and the fibers of polyester (PET/PBT) of P1. Moreover, the polyester fibers P2 are smooth and thicker than P1 with an average fiber diameter of 6  $\mu\text{m}$ .

According to the data sheets, the nonwoven polyester based on PET/PBT has higher mechanical strength (200 N/5 cm), lower thickness (120  $\mu\text{m}$ ), and weight of 85  $\text{g m}^{-2}$  compared with the polyester based on PET, which has lower mechanical strength (120 N/5 cm), higher thickness

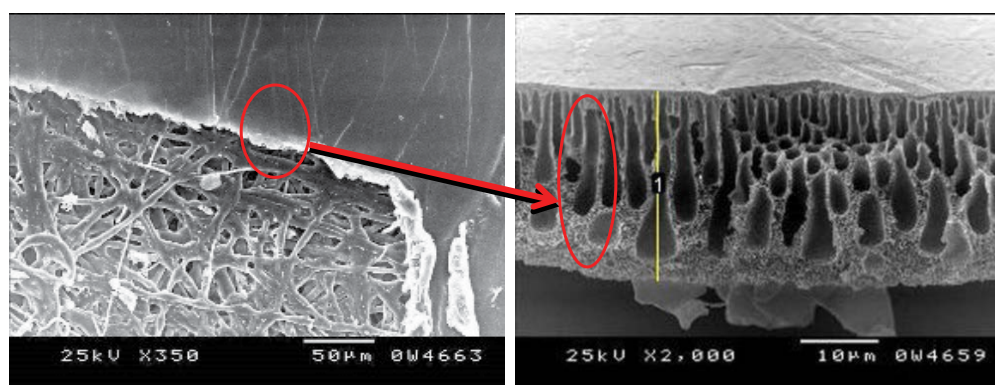


Fig. 4. SEM images of the cross section of the PS membrane supported on nonwoven polyester P1.



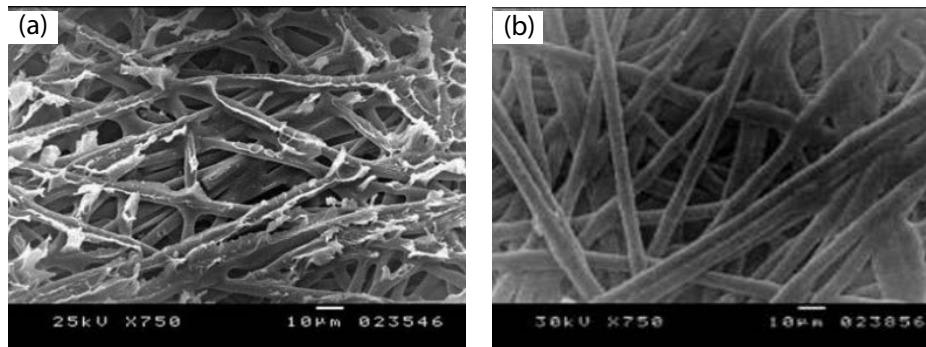


Fig. 5. SEM images of the bottom surface of the PS membranes supported on polyester (a) P1 and (b) P2.

(130  $\mu\text{m}$ ), and weight of  $70 \text{ g m}^{-2}$ . Blending of PET/PBT offers superior mechanical and thermal properties than using PET alone [17]. As a result, the P1 is chosen to be examined at the different coagulation times, and its optimum performance condition will be compared with the performance of P2.

### 3.2. Effect of coagulation time on the morphology of the PS membrane supported on nonwoven polyester fabric

The effect of the coagulation time on the top surface topography of the prepared PS-supported membrane P1 is shown in Fig. 6. At coagulation time of 10 and 30 min, the images presented in Figs. 6(a) and (b) have few blocked pores which are formed on the surface of the membranes due to the presence of the air bubbles and they have disappeared by increasing the coagulation time to 60 and 120 min. In addition, the smooth surfaces shown in images Figs. 6(c)

and (d) are attributed to the complete solidification of the polymer solution without surface defects.

As shown in Fig. 7, the cross section of the PS membranes supported with P1 consists of a finger-like structure and these fingers become narrow with macrovoid formation with increase in coagulation time. When the polyester fabric is wet with NMP, a barrier of the solvent film is formed on the bottom and this greatly delays the nonsolvent diffusion into the casting solution and consequently leads to a delayed de-mixing. This delayed de-mixing is one of the main driving forces for macrovoid formation [18], and increasing the coagulation time enhances the formation of macrovoids. Also, increasing the coagulation time, for more than 30 min, causes an increase in the thickness of the skin layer, which forms a resistance for the flow of water inside the pores of the membrane and consequently affects the performance of the TFC membranes.

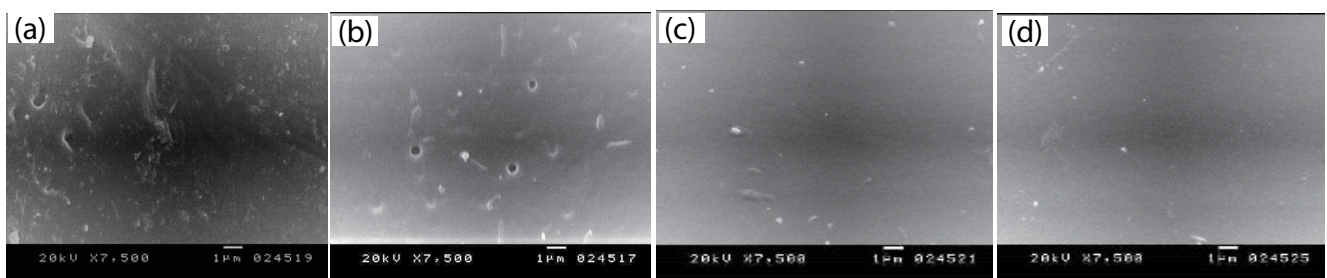


Fig. 6. SEM images of the surface of the PS supported on polyester P1 at different coagulation times of (a) 10 min, (b) 30 min, (c) 60 min, and (d) 120 min.

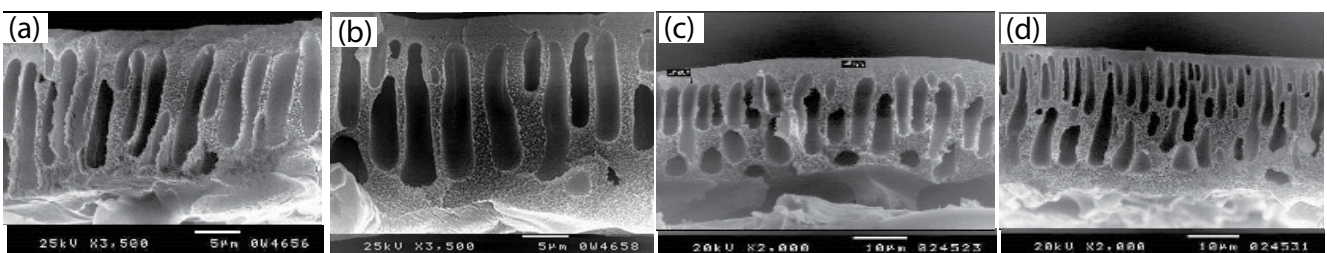


Fig. 7. SEM images of the cross sections of the PS supported on polyester at different coagulation times (P1) (a) 10 min, (b) 30 min, (c) 60 min, and (d) 120 min.

Fig. 8 shows the bottom of the PS-supported membranes (P1) with different coagulation times. At low coagulation times of 10 and 30 min, the PS solution is partially wetted and penetrated the bottom of the polyester fibers to form the white lumps. On the other hand, the PS membrane has fully coated the bottom surface of the polyester fibers at coagulation times of 60 and 120 min [19].

Fig. 9 depicts the SEM image of the cross section of the full layers of TFC RO membrane at coagulation time of 30 min. The TFC membrane consists of very thin PA layer on PS membrane (with thickness of 25  $\mu\text{m}$ ) supported on nonwoven polyester fabric (with thickness of 120  $\mu\text{m}$ ). Also, the fibers of the polyester are compacted and overlapped. It is difficult technically to take SEM images of the full TFC membrane layers at different coagulation times because the cutting of the cross section affects the finger-like structure.

### 3.3. The effect of coagulation time on the performance of TFC1 RO membranes

There is a large difference between the casting thickness and the final membrane thickness. This implies that during the membrane formation process, the boundary between the nonsolvent bath and the casting solution moves downward, as shown in Fig. 10. As the immersion process starts at  $T = 0$ , the solvent will diffuse out of the film and the nonsolvent will diffuse in. This process will continue until the equilibrium is reached at time  $T = t$ , and the membrane is formed [20].

The square of the boundary layer movement distance ( $x^2$ ) is linearly proportional to coagulation time; therefore, the diffusion kinetics in the phase inversion reaction is conformed to the Fickian Diffusion Law. Afterward, Kang et al. derived the following Eq. (1):

$$X^2 = 4 \times D_c \times t \quad (1)$$

where  $X$  is the moved distance of the boundary layer (mm),  $D_c$  is the diffusion coefficient ( $\text{mm}^2 \text{s}^{-1}$ ), and  $t$  is the coagulation time (s) [21]. This equation indicates that the coagulation time will greatly affect the performance of the membranes due to the change in the surface structure and the morphology of the TFC membranes [18]. The performance of the prepared TFC1 membranes was evaluated by measuring both the permeate flux ( $\text{L m}^{-2} \text{h}^{-1}$ ) and the salt rejection (%) at different coagulation times as shown in Fig. 11. The water flux has decreased by increasing the coagulation time above 30 min.

Because the pores are the least mechanically stable regions of a membrane and the macrovoid walls respond greatly to the applied pressures, thus as the pressure is applied, the pore walls become denser and the macrovoids become smaller, resulting in an increase in the hydraulic resistance and a decrease in the flux across the membrane.

On the other hand, the salt rejection has slightly increased with increasing coagulation time, but the rejection has sharply decreased beyond a coagulation time of 60 min with increase in the flux. This may be due to the formation of macrovoids, which cannot stand the high pressure and leading to an increase of the water and the salt transport across the membrane. The highest performance for the prepared TFC1 membrane is obtained at a coagulation time equal to 30 min, which produces the best flux ( $47 \text{ L m}^{-2} \text{h}^{-1}$ ) and rejection (98%).

### 3.4. Comparison between the performance of the prepared TFC membranes and the TFC-St membranes

The P1 membrane was prepared at the optimum coagulation time of 30 min. As shown in Figs. 12 and 13, the performance of the prepared TFC1 RO membrane ( $47.6 \text{ L m}^{-2} \text{h}^{-1}$ , 98%) is higher than the performance of the TFC2 ( $23.8 \text{ L m}^{-2} \text{h}^{-1}$ , 92.6%), and these results confirm that using PET/PBT fabric (P1 polyester) is better than PET alone (P2) as mentioned

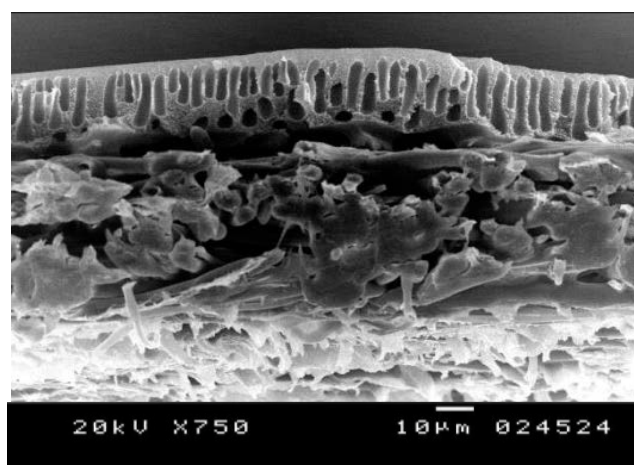


Fig. 9. SEM image of the cross section of the full layers of TFC membrane at coagulation time of 30 min.

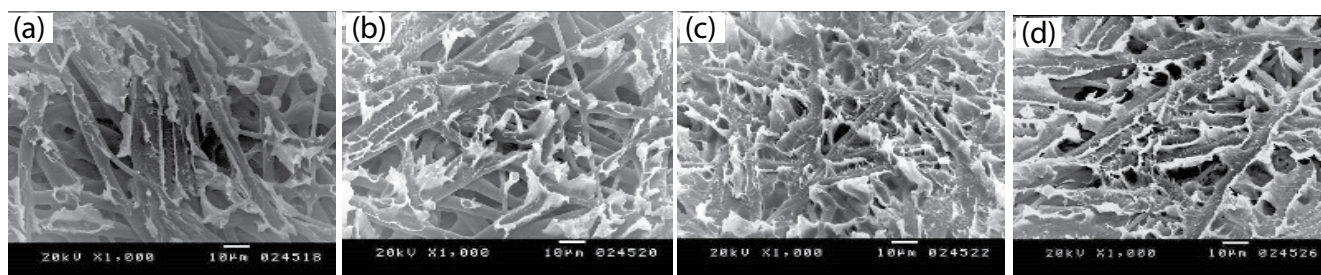


Fig. 8. SEM images of the bottom surfaces of the PS membranes supported onto polyester (P1) with coagulation times of (a) 10 min, (b) 30 min, (c) 60 min, and (d) 120 min.

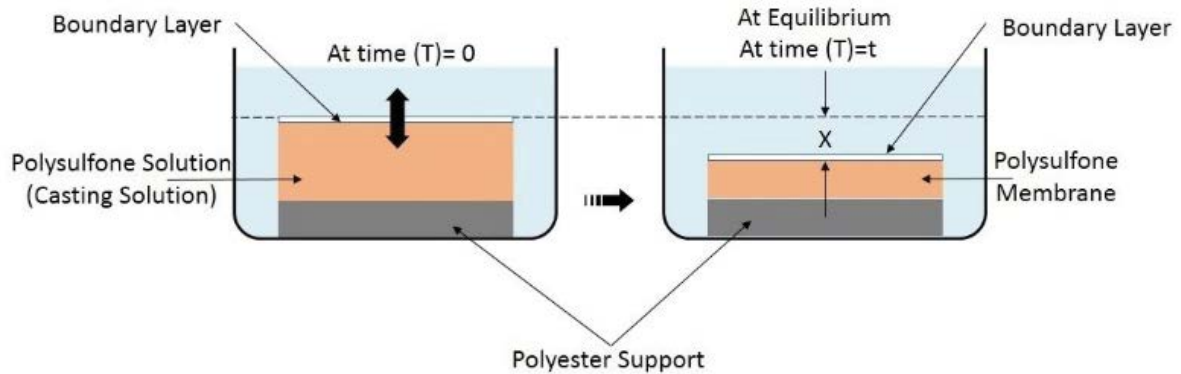


Fig. 10. Schematic representation of the immersion process of the membrane at different times.

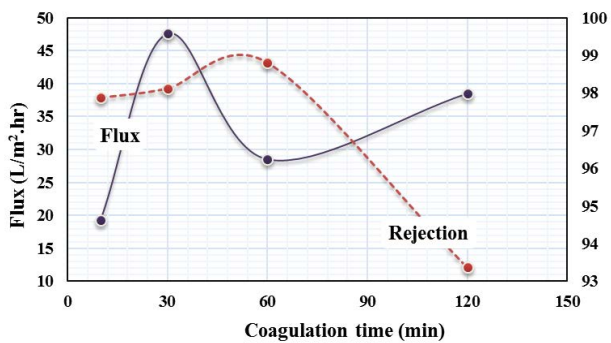


Fig. 11. The water flux and the salt rejection of the prepared TFC1 membrane versus coagulation time at 55 bar.

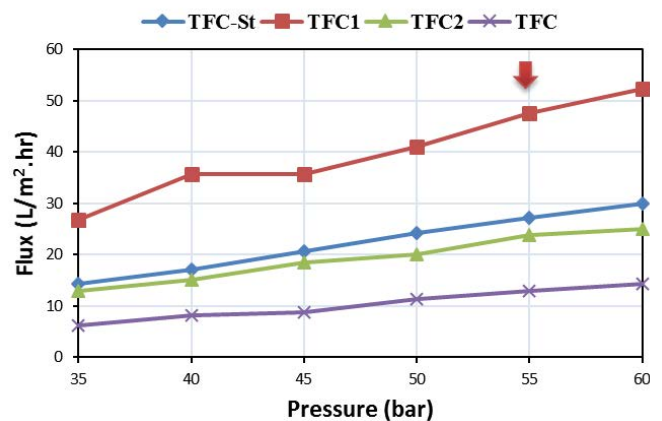


Fig. 13. Water flux vs. operating pressure of TFC RO membranes at 55 bar.

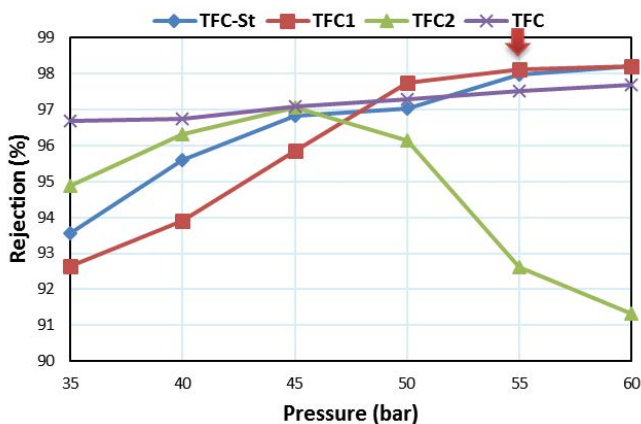


Fig. 12. Salt rejection vs. operating pressure of TFC RO membranes at 55 bar.

in section 3.1. In addition, the prepared TFC1 membrane produces better performance than the TFC-St membrane ( $27 \text{ L m}^{-2} \text{ h}^{-1}$ , 97.9%). The TFC membrane (without nonwoven polyester) produces the lowest performance ( $10 \text{ L m}^{-2} \text{ h}^{-1}$ , 97%) because the thickness of the prepared PS membrane has a high resistance to the transport of water.

Also, it is observed that the water flux and the salt rejection of the PA-RO membranes increase with increasing the operating pressure. As the pressure increases, the driving force for the solvent transport increases; hence, more amount of water can be transported through the membrane with high salt rejection (i.e., the remaining (nonrejected) salt in the permeate is fixed but the amount of water permeate increases, so the permeate is diluted and the percent salt rejection increases) [22].

#### 4. Conclusions

The coagulation time had a great effect on the performance of the TFC membranes, which were prepared by the IP of MPD and TMC on the surface of the PS membrane supported on nonwoven polyester fabric. SEM images revealed that the pore characteristics are dependent on the coagulation time. The optimum coagulation time was found to be 30 min. The performance of TFC membranes was affected by the support layers; the performance of TFC1 supported on PET/PBT produced values of water flux of  $47.6 \text{ L m}^{-2} \text{ h}^{-1}$  and rejection of 98%, which were high compared with the performance of TFC2 membrane supported on PET ( $23.8 \text{ L m}^{-2} \text{ h}^{-1}$ , 92.6%), the TFC-St ( $27 \text{ L m}^{-2} \text{ h}^{-1}$ , 98%), and the TFC without nonwoven polyester ( $10 \text{ L m}^{-2} \text{ h}^{-1}$ , 97%).



## Acknowledgment

This work was supported by the Egyptian Science and Technology Development Fund, (grant numbers 3988).

## References

- [1] K.P. Lee, T.C. Arnot, D. Mattia, A review of reverse osmosis membrane materials for desalination-development to date and future potential, *J. Membr. Sci.*, 370 (2011) 1–22.
- [2] A. Khalifa, H. Ahmad, M. Antar, T. Laoui, M. Khayet, Experimental and theoretical investigations on water desalination using direct contact membrane distillation, *Desalination*, 404 (2017) 22–34.
- [3] M. Schouppe, Membrane technologies for water applications, European Research Projects, EUR 24552 EN, 2010, 40.
- [4] K. Zotalis, E.G. Dyalynas, N. Mamassis, A.N. Angelakis, Desalination technologies: hellenic experience, *Water*, 6 (2014) 1134–1150.
- [5] F.M. Khour, Multistage Separation Processes, 3rd Ed., CRC Press, Florida, 2005, pp. 440–461.
- [6] T. Humplik, J. Lee, S.C.O. Hern, B.A. Feeman, M.A. Baig, S.F. Hassan, M.A. Atieh, F. Rahman, T. Laoui, R. Karnik, E.N. Wang, Nanostructured materials for water desalination, *Nanotechnology*, 22 (2011) 1–19.
- [7] R. Verbeke, V. Gómez, I.F.J. Vankelecom, Chlorine-resistance of reverse osmosis (RO) polyamide membranes, *Program Polym. Sci.*, 72 (2017) 1–15.
- [8] N. Misdan, W.J. Lau, A.F. Ismail, Seawater reverse osmosis (SWRO) desalination by thin-film composite membrane—current development, challenges and future prospects, *Desalination*, 287 (2012) 228–237.
- [9] M. Di Vincenzo, M. Barboiu, A. Tiraferri, Y.M. Legrand, Polyol-functionalized thin-film composite membranes with improved transport properties and boron removal in reverse osmosis, *J. Membr. Sci.*, 540 (2017) 71–77.
- [10] N. Misdan, W.J. Lau, A.F. Ismail, T. Matsuura, Formation of thin film composite nanofiltration membrane: effect of polysulfone substrate characteristics, *Desalination*, 329 (2013) 9–18.
- [11] C. Ding, J. Yin, B. Deng, Effects of polysulfone (PSf) support layer on the performance of thin-film composite (TFC) membranes, *J. Chem. Process Eng.*, 1 (2014) 1–8.
- [12] M.E. Yakavangi, S. Rimaz, V. Vatanpour, Effect of surface properties of polysulfone support on the performance of thin film composite polyamide reverse osmosis membranes, *J. Appl. Polym. Sci.*, 134 (2017) 44444–44453.
- [13] M. Said, S. Ebrahim, A. Gad, S. Kandil, Performance and stability of diaminotoluene-based polyamide composite reverse osmosis membranes incorporated with additives and cast on polyester fabric, *Desal. Wat. Treat.*, 86 (2017) 115–123.
- [14] H. Strathmann, Production of Micro-porous Media by Phase Inversion Processes, American Chemical Society, Washington, DC, 1985, pp. 1–31.
- [15] M. Sarif, Development of integrally skinned polysulfone ultrafiltration membrane: effect of casting parameters, M.Sc. Dissertation, University Sains, Malaysia, 2005.
- [16] B.D. Coday, T. Luxbacher, A.E. Childress, N. Almaraz, P. Xu, T.Y. Cath, Indirect determination of zeta potential at high ionic strength: specific application to semipermeable polymeric membranes, *J. Membr. Sci.*, 478 (2015) 58–64.
- [17] R.N. Baxi, S.U. Pathak, D.R. Peshwe, Impact modification of a PET–PBT blend using different impact modifiers, *Polymer J.*, 43 (2011) 801–808.
- [18] R.X. Zhang, J. Vanneste, L. Poelmans, A. Sotto, X.L. Wang, B. Van der Bruggen, Effect of the manufacturing conditions on the structure and performance of thin-film composite membranes, *J. Appl. Polym. Sci.*, 125 (2012) 3755–3769.
- [19] F.J. Tsai, D. Kang, M. Anand, Thin-film-composite gas separation membranes: on the dynamics of thin film formation mechanism on porous substrates, *Sep. Sci. Technol.*, 30 (1995) 1639–1652.
- [20] M. Mulder, Basic Principles of Membrane Technology, 2nd Ed., Kluwer Academic Publishers, Dordrecht, London, 1997.
- [21] Q.-Z. Zheng, P. Wang, Y.-N. Yang, Rheological and thermodynamic variation in polysulfone solution by PEG introduction and its effect on kinetics of membrane formation via phase-inversion process, *J. Membr. Sci.*, 279 (2006) 230–237.
- [22] V.V. Gedam, J.L. Patil, S. Kagne, R.S. Sirsam, P. Labhasetwar, Performance evaluation of polyamide reverse osmosis membrane for removal of contaminants in ground water collected from Chandrapur District, *J. Membr. Sci. Technol.*, 2 (2012) 1–5.